Journal of Multidisciplinary Engineering Science and Technology (JMEST)
ISSN: 2458-9403
Vol. 8 Issue 6, June - 2021

ANALYSIS OF HIGH ELEVATION HILL AND PLATEAU TERRAIN IMPACT ON NONE LINE-OF-SIGHT WIRELESS COMMUNICATION LINKS

Osuji Dennis Chiazor[2]
Department of Space Education and Training, Advanced Space Technology Applications Laboratory, Uyo, Akwa Ibom, Nigeria
dennischiazor@gmail.com

Itoro Obot[2]
Department of electrical and electronic engineering,
Nigerian Army University, Biu Nigeria.
Itobot55@yahoo.com

Okafor Brian Okwuchukwu[3]
Department of Space Applications and Research, Advanced Space Technology Applications Laboratory, Uyo, Akwa Ibom, Nigeria
bokafor@astaluyo.gov.ng

***Abstract*— In this paper, evaluation of high elevation hill and plateau terrain impact on none line-of-sight wireless communication links is presented. The shape of the hilly and plateau path profiles are defined by the ratio of the path profile occultation distance and the path length of the wireless communication link. The International Telecommunication Union (ITU) parabola method is used to determine the required radius of curvature for any given hilly and plateau path profile while the Recommendation ITU-R P.526-13 method is used to calculate the rounded edge diffraction loss proffered by the given hilly and plateau path profile. The path profile data of a case study hilly terrain used is such that the transmitter x,y coordinates are 0, 343.9 respectively, the receiver x,y coordinates are 7283.4, 286.7 respectively, while the maximum elevation of 469.1528 m occurred at a distance of 3249.74 m from the transmitter with the coordinates of 3249.74,469.1528 respectively.The computation of the rounded edge radius of curvature and the rounded edge diffraction loss was implemented in Matlab software using the following values of ratio of the occultation distance to the path length , β = 0.32, β = 0.4910, β = 0.5634 and β = 0.92. The results show that when β = 0.32, the radius of curvature is 8,446.01 m while the computed rounded edge diffraction loss, G(dB) is 50.64527 dB. Again, when β = 0.92, the obstacle profile is a plateau and the radius of curvature is 78,451.83 m while the computed rounded edge diffraction loss, G(dB) is 1212.741 dB. Furthermore, quadratic analytical models were developed for estimating the radius of curvature and the rounded edge diffraction loss for the case study terrains. In all, the results showed that plateau terrains require larger radius of curvature and hence present larger diffraction loss value to the wireless signal than the hilly terrain.**

Keywords*— *Hill Terrain, Diffraction Loss, Plateau Terrain, Wireless Signal, Occultation Distance , Wireless Communication, Path Length

1. INTRODUCTION

Telecommunication entails communication over a distance where the transmitter and the receiver are separated by a certain distance but are connected by a certain communication medium [1,2,3,4,5,6]. In the case of terrestrial wireless communication system, the communication medium is the atmosphere [7,8,9,10]. In such case, the wireless signals suffer several losses due to atmospheric parameters such as rain and fog [11,12,13,14,15,16,17]. Also, there is the inevitable signal spreading loss referred to as free space path loss [18,19,20,21,22]. Furthermore, there is loss due to obstructions in the signal path [23,24,25]. Such obstruction can be trees, building of high rising structures. Also, earth topological features such as high elevation mountains and plateaus can also constitute an obstruction to the signal.

Generally, obstructions in the signal path can cause diffraction loss [23, 24, 25, 26, 27, 28, 29, 30, 31]. Isolated obstructions are generally modeled as single knife edge obstruction or rounded edge obstruction. Rounded edge obstruction are often used for high elevation hills and plateaus that are relatively large in size when compared with the path length of the communication link. However, the diffraction loss differ with different shapes of the high elevation obstruction.

Accordingly, in this paper, analysis of the impact of high elevation hills and plateaus on the rounded edge diffraction loss suffered by signal in a wireless communication system is presented. The hilly and plateau obstructions are identified by the ratio of the occultation distance to the path length of the communication link. Particularly, the rounded edge diffraction loss is computed using the International Telecommunication Union (ITU) Recommendation ITU-R P.526-13 method. In all, the study seeks to demonstrate how different earth surface topographical features affect wireless communication system.

2. METHODOLOGY

2.1 The effect of occultation distance

Consider the transmitter and receiver separated by a distance with path length of d (km) and there exist an obstacle in the signal path between the transmitter and the receiver, as shown in Figure 1. The obstruction can cause diffraction loss. There are different diffraction loss models that can be applied to estimate the loss due to diffraction. There is single knife edge diffraction loss model, double single and multiple single knife edge diffraction loss models, as well as rounded edge diffraction loss model. The specific model to be employed depends on the nature of the obstacle.

In practice, a typical round edge obstruction is a hilly terrain in the path of the signal. Such hilly terrain is defined by the path profile of the terrain. Accordingly, a typical hilly path profile used for the analysis of the rounded edge diffraction loss is presented in Figure 1. The two key parameters used to define the shape of the hilly path profile are the occultation distance (D_{occ}) and the path length (d), as shown in Figure 1.

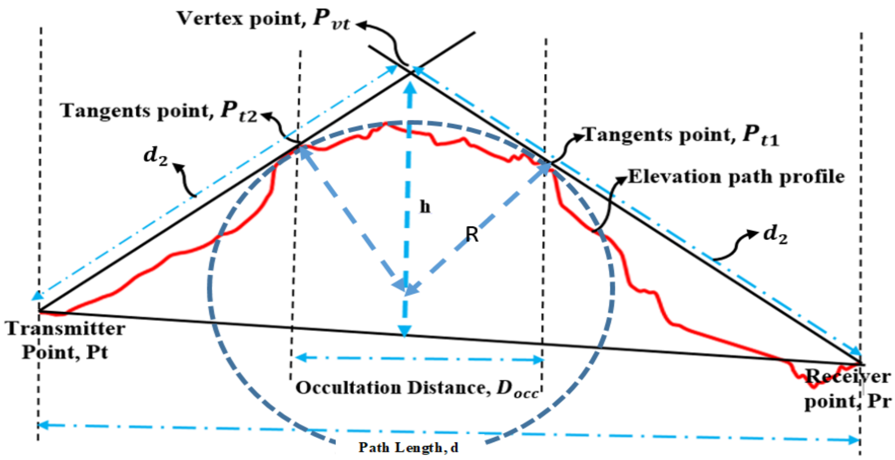

Figure 1 A typical hilly terrain path profile (in red colour) used for the analysis of the rounded edge obstacle

Let β be the ratio of the occultation distance (D_{occ}) to the path length (d), hence,

$$\beta = \frac{D_{occ}}{d} \quad (1)$$

When D_{occ} is zero, hence $\beta = 0$; in this case, the terrain is a knife edge obstruction and hence, the knife edge diffraction loss model is used. When $D_{occ} = d$, hence $\beta = 1$. In this case, the terrain is a flat plane or plateau. The rounded edge can still be applied to estimate the diffraction loss of such terrain. In practice, the rounded edge diffraction loss model is applied when $0 < \beta < 1$. This covers the hilly terrains as well as the plateau terrains. In this paper, the single rounded edge diffraction loss is estimated using the International Telecommunication Union (ITU) Recommendation ITU-R P.526-13 method.

2.2 The ITU-R P.526-13 method of calculating the diffraction loss over single rounded edge obstruction

When the path profile of any obstruction is such that $0 < \beta < 1$, a rounded edge can be fitted towards the vicinity of the obstruction apex. The radius of the rounded edge fitted to the obstruction is then used in the estimation of the rounded edge diffraction loss. The geometry used for the analysis of the rounded edge obstacle and their associated rounded edge diffraction loss is given in Figure 2.

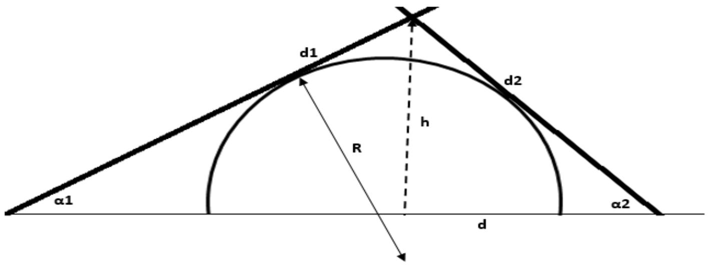

Figure 2 The geometry used for the analysis of the rounded edge obstacle and their associated rounded edge diffraction loss

Where in Figure 2, d_1 and d_2 are the length (in kilometers) of the tangent lines drawn from the transmitter and the receiver, R is the radius of the circle that is fitted to the path profile of the obstacle and h is the clearance height in meters for the computation of the diffraction loss. The rounded edge diffraction loss (A_{dB}) according to the ITU-R method is given as;

$$A_{dB} = J(\nu) + T(m, n) \quad (2)$$

where J(ν) denotes the Fresnel-Kirchoff diffraction loss due to an equivalent single knife-edge obstruction that has its peak at the vertex point. The dimensionless Fresnel-Kirchoff diffraction parameter, ν is evaluated as:

$$\nu = 0.0316(h)\left[\sqrt[2]{\left(\frac{2(d_1 + d_2)}{\lambda(d_1)(d_2)}\right)}\right] \quad (3)$$

where λ is signal wavelength in meters d_1 and d_2 are in kilometers. Then, J(ν) and $T(m,n)$ are computed as follows;

$$J(\nu) = 6.9 + 20\log\left(\left(\sqrt{(\nu - 0.1)^2 + 1}\right) + \nu - 0.1\right) \quad (4)$$

$$T(m,n) = k(m)^b \quad (5)$$

where:

$$k = 8.2 + 12\,(n) \quad (6)$$

$$b = 0.73 + 0.27\left[1 - e^{(-1.43\,(n))}\right] \quad (7)$$

and:

$$m = (R)\left[\frac{(d_1 + d_2)}{d_1 d_2}\right] \Big/ \left[\frac{\pi R}{\lambda}\right]^{1/3} \quad (8)$$

$$m = h\left[\frac{\pi R}{\lambda}\right]^{2/3}(R) \quad (9)$$

2.2 RADIUS OF CURVATURE BY THE INTERNATIONAL TELECOMMUNICATION UNION (ITU) PARABOLA METHOD

In the ITU Parabola method, the radius of curvature is computed from the vertical profile data of the path, (Figure 3). If there are n elevation sample points, the mean radius of curvature by ITU Parabola method is given as:

$$R = \frac{1}{n}\left[\sum_{i=1}^{i=n}\left(\frac{x_i^2}{2Y_i}\right)\right] \quad (10)$$

where

$$r_i = \frac{x_i^2}{2Y_i} \quad (11)$$

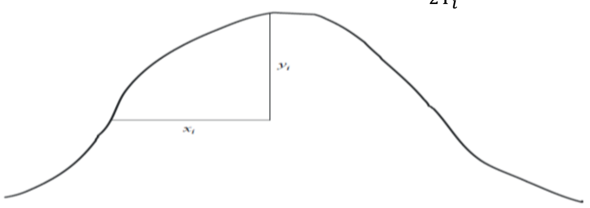

Figure 3: The parameters for the ITU Parabola method

The radius of the first Fresnel Zone is used to determine the range of path profile elevation data that is considered in the ITU parabola method. The radius of the first Fresnel Zone required to determine the limit of Y_i and x_i is computed as follows;

$$R_{fr} = 17.32\left(\sqrt{\frac{(d_t)(d_r)}{f(d_t+d_r)}}\right) \quad (12)$$

Where R_{fr} denotes the Fresnel zone radius in metres; d_t denotes the distance of transmitter antenna to the point of obstruction; d_t is in km; d_r denotes the distance of receiver antenna to the point of obstruction, d_r is in km and f denotes the frequency in GHz .

2.3 The Case Study Path Profile

A portion of the case study elevation profile dataset is presented in Table 1 and the path profile plot is presented in Figure 4. The path profile data of the case study hilly terrain is such that the transmitter x,y coordinates are 0, 343.9, the receiver coordinates are 7283.4, 286.7 while the maximum elevation of 469.1528 m occurred at a distance of 3249.74 m from the transmitter with the coordinates of 3249.74,469.1528.

Table 1: The Elevation Profile Data for the Case Study Hilly Terrain

Distance (m)	Elevation (m)	Distance (m)	Elevation (m)	Distance (m)	Elevation (m)	Distance (m)	Elevation (m)	Distance (m)	Elevation (m)
0	343.9	1282.8	389.2	2565.6	456.2	3848.4	453.8	5131.2	382.8
42.8	346.1	1325.6	389.7	2608.3	454.8	3891.1	454.5	5173.9	379.7
128.3	349	1411.1	390.5	2693.9	454.2	3976.7	451	5259.4	369.4
213.8	351.1	1496.6	392.2	2779.4	456.6	4062.2	448.4	5345	347
299.3	355	1582.1	394.7	2864.9	459.2	4147.7	444.4	5430.5	345
342.1	356.4	1624.9	396.4	2907.7	460.3	4190.5	442.7	5473.2	343.3
427.6	358.7	1710.4	400.7	2993.2	461.8	4276	440	5587.3	328.5
470.4	359.7	1753.1	401	3035.9	460.2	4318.7	438.4	5644.3	321.5
555.9	361.5	1838.7	403.1	3121.5	465	4404.3	439.5	5758.3	317.9
598.6	362.8	1881.4	405.3	3164.2	465	4447	442.4	5815.3	315.6
684.2	364.4	1966.9	410.2	3249.7	469.2	4532.5	436.1	6699	284.8
726.9	365.9	2009.7	412.7	3292.5	467.3	4575.3	435.8	6741.8	279.6
812.4	369.9	2095.2	419.1	3378	464.2	4660.8	430.5	6827.3	276.4
898	374.5	2180.7	428.6	3463.5	462.4	4746.3	407.9	6912.8	275.2
983.5	377.7	2266.3	447	3549.1	461	4831.9	400.8	6998.3	277.2
1026.2	378.9	2309	450	3591.8	460.1	4874.6	397.4	7041.1	278.5
1111.8	382	2394.5	453.6	3677.3	453.1	4960.1	390.7	7126.6	285.2
1154.5	384.1	2437.3	455.4	3720.1	453	5002.9	388.3	7169.4	283.2
1240	388.5	2522.8	456.9	3805.6	453.3	5088.4	384.2	7283.4	286.7

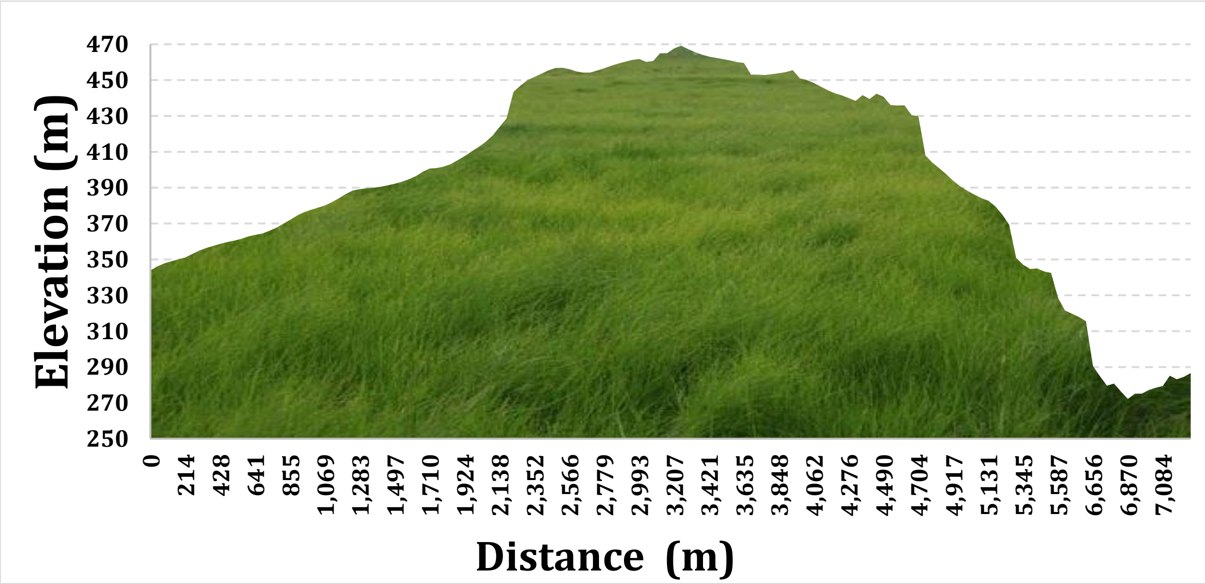

Figure 4. The elevation versus distance plot (that is, the path profile plot) of the case study hilly terrain

3. RESULTS AND DISCUSSION

The computation of the rounded edge radius of curvature and the rounded edge diffraction loss was implemented in Matlab software using the following values of the ratio of the occultation distance (D_{occ}) to the path length (d), β = 0.32, β = 0.4910, β = 0.5634 and β = 0.92 . The sketch of the case study rounded edge high elevation path profile for the occasion where β = 0.32 is given in Figure 5. The image in Figure 5 shows that when β = 0.32 the obstacle profile is a hill. The results show that when β = 0.32, the radius of curvature is 8,446.01 m while the computed rounded edge diffraction loss, G(dB) is 50.64527 dB. Again, the sketch of the case study rounded edge high elevation path profile for the occasion where β = 0.92 is given in Figure 6. The image in Figure 6 shows that when β = 0.92 the obstacle profile is a plateau. Also, the results show that when β = 0.92, the radius of curvature computed by ITU method is 78,451.83 m while the computed rounded edge diffraction loss, G(dB) is 1212.741 dB.

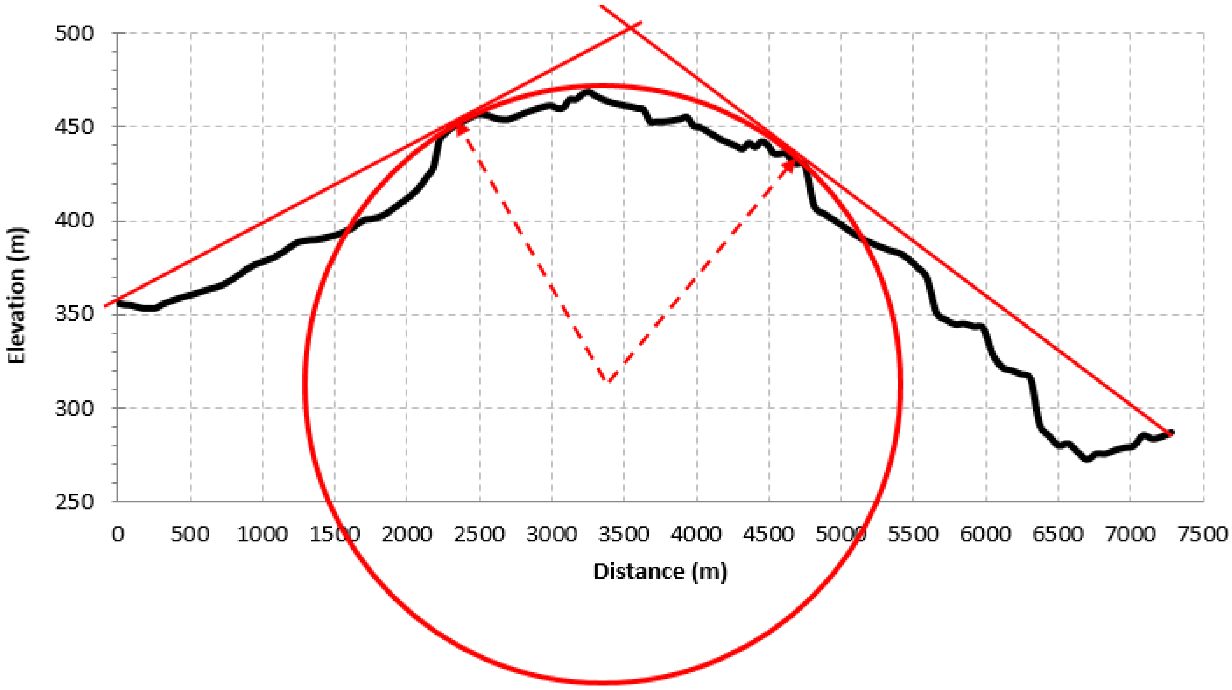

Figure 5 The sketch of the case study rounded edge high elevation path profile for the occasion where β = 0.32

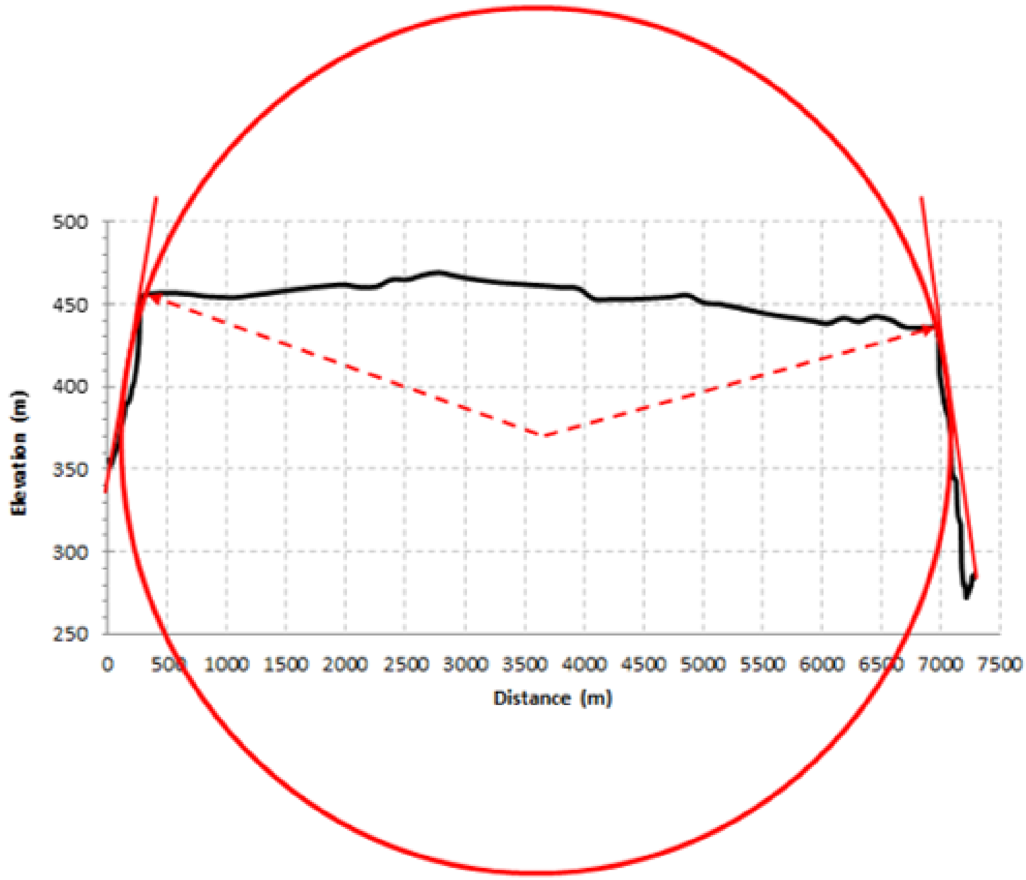

Figure 6 The sketch of the case study rounded edge high elevation path profile for the occasion where β = 0.92

The analysis was conducted for other values of β = 0.4910 and β = 0.5634 and the results for all the four different cases of β considered in the study are shown in Table 2. A graph of the radius of curvature, R (m) versus β is given in Figure 7. The graph gave a quadratic expression for approximating the radius of curvature for the case study high elevation profile as a function of β, as follows;

$$R\ (m) = 95339\beta^2 - 1546.3\beta - 820.85 \quad (13)$$

Similarly, a graph of the rounded edge diffraction loss G(dB) versus β is given in Figure 8. The graph gave a quadratic expression for approximating G(dB) for the case study high elevation profile as a function of β as follows;

$$G(dB) = 4311.8\beta^2 - 3421.9\beta + 709.78 \quad (14)$$

The results in Table 2 shows that as the value of β increases , the radius of curvature, R (m) and also the rounded edge diffraction loss G(dB) increases. Notably, the higher the value of β the more the profile turns to a plateau with flat top and the smaller the value of β the more the profile turns to a knife edge . For the cases in Table 2 where β = 0.32, β = 0.4910 and β = 0.5634 , the obstacle profile showed hilly terrain. As such, the results showed that plateau requires larger radius of curvature and hence presents higher rounded edge diffraction loss than hilly obstacle.

Table 2 Rounded edge radius of curvature, R (m) and the Rounded Edge Diffraction G(dB) Loss (dB) for the four cases of β = 0.32, β = 0.4910, β = 0.5634 and β = 0.92

β	**Radius of curvature, R (m)**	**Rounded Edge Diffraction Loss G(dB))**
0.32	8,446.01	50.64527
0.4910	21,409.32	95.82028
0.5634	28,566.27	128.0203
0.92	78,451.83	1212.741

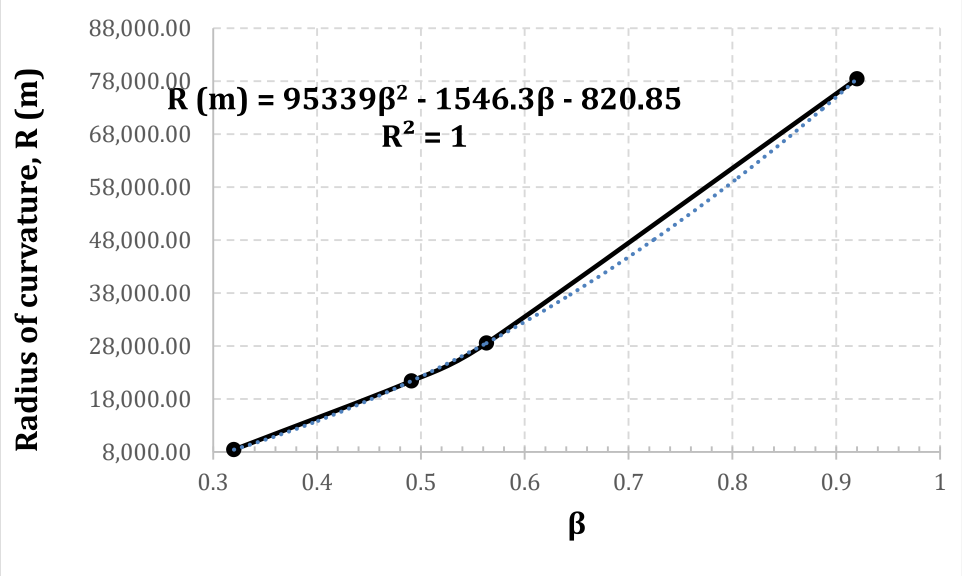

Figure 7 graph of the radius of curvature, R (m) versus **β**

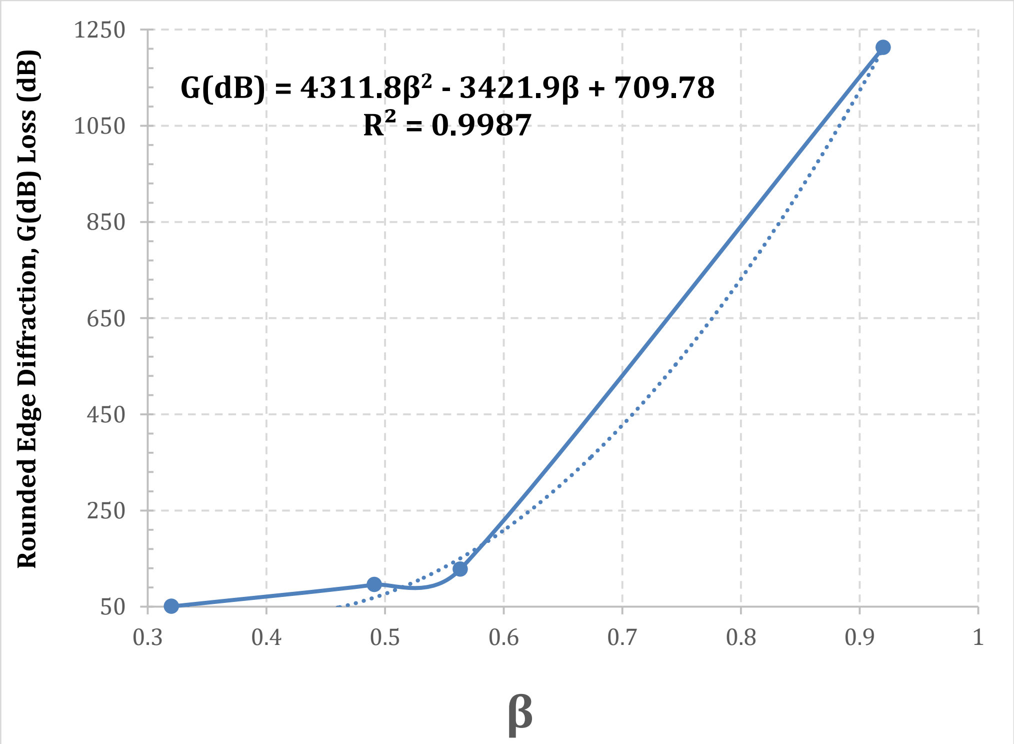

Figure 8 The graph of the rounded edge diffraction loss G(dB) versus **β**

4. CONCLUSION

The effect of high elevation hilly and plateau terrains on the diffraction loss suffered by signals of wireless communication systems is presented. The path profiles of different high elevation terrain containing hills and plateaus are used to determine the radius of curvature of the rounded edge and hence the rounded edge diffraction loss due to each of the different profile shape. The results showed that plateau terrains require larger radius of curvature and hence present larger diffraction loss value to the wireless signal than the hilly terrain. Furthermore, quadratic analytical models were presented for estimating the radius of curvature and the rounded edge diffraction loss for the case study terrains.

REFERENCES

1. Siegel, T., & Chen, S. P. (2021). Investigations of Free Space Optical Communications under Real-World Atmospheric Conditions. *Wireless Personal Communications*, *116*(1), 475-490.
2. Bi, S., Zeng, Y., & Zhang, R. (2016). Wireless powered communication networks: An overview. *IEEE Wireless Communications*, *23*(2), 10-18.

3. Sadiku, M. N. (2018). *Optical and wireless communications: Next generation networks*. CRC press.
4. Basar, E., Di Renzo, M., De Rosny, J., Debbah, M., Alouini, M. S., & Zhang, R. (2019). Wireless communications through reconfigurable intelligent surfaces. *IEEE access*, *7*, 116753-116773.
5. Willner, A. E., Huang, H., Yan, Y., Ren, Y., Ahmed, N., Xie, G., ... & Ashrafi, S. (2015). Optical communications using orbital angular momentum beams. *Advances in Optics and Photonics*, *7*(1), 66-106.
6. Staniec, K., & Habrych, M. (2016). Telecommunication platforms for transmitting sensor data over communication networks—state of the art and challenges. *Sensors*, *16*(7), 1113.
7. Siles, G. A., Riera, J. M., & Garcia-del-Pino, P. (2015). Atmospheric attenuation in wireless communication systems at millimeter and THz frequencies [Wireless Corner]. *IEEE Antennas and Propagation Magazine*, *57*(1), 48-61.
8. Holfeld, B., Wieruch, D., Wirth, T., Thiele, L., Ashraf, S. A., Huschke, J., ... & Ansari, J. (2016). Wireless communication for factory automation: An opportunity for LTE and 5G systems. *IEEE Communications Magazine*, *54*(6), 36-43.
9. Chien, W. C., Lai, C. F., Hossain, M. S., & Muhammad, G. (2019). Heterogeneous space and terrestrial integrated networks for IoT: Architecture and challenges. *IEEE Network*, *33*(1), 15-21.
10. Yu, X., Han, W., & Zhang, Z. (2017). Path loss estimation for wireless underground sensor network in agricultural application. *Agricultural Research*, *6*(1), 97-102.
11. Amarasinghe, Y., Zhang, W., Zhang, R., Mittleman, D. M., & Ma, J. (2020). Scattering of terahertz waves by snow. *Journal of Infrared, Millimeter, and Terahertz Waves*, *41*(2), 215-224.
12. Rashed, A. N. Z. (2014). High efficiency wireless optical links in high transmission speed wireless optical communication networks. *International Journal of Communication Systems*, *27*(11), 3416-3429.
13. Niaz, A., Qamar, F., Ali, M., Farhan, R., & Islam, M. K. (2019). Performance analysis of chaotic FSO communication system under different weather conditions. *Transactions on Emerging Telecommunications Technologies*, *30*(2), e3486.
14. Singh, M., Malhotra, J., Rajan, M. M., Dhasarathan, V., & Aly, M. H. (2020). Performance evaluation of 6.4 Tbps dual polarization quadrature phase shift keying Nyquist-WDM superchannel FSO transmission link: Impact of different weather conditions. *Alexandria Engineering Journal*, *59*(2), 977-986.
15. Taherkhani, M., Kashani, Z. G., & Sadeghzadeh, R. A. (2020). On the performance of THz wireless LOS links through random turbulence channels. *Nano Communication Networks*, *23*, 100282.
16. Islam, S. (2020). Atmospheric Propagation Impairment Effects for Wireless Communications. *International Journal of Wireless & Mobile Networks (IJWMN) Vol*, *12*.
17. Maswikaneng, S. P., Owolawi, P. A., Ojo, S. O., & Mphahlele, M. I. (2018, December). Atmospheric effects on free space optics wireless communication: applications and challenges. In *2018 International Conference on Intelligent and Innovative Computing Applications (ICONIC)* (pp. 1-5). IEEE.
18. Tang, W., Chen, M. Z., Chen, X., Dai, J. Y., Han, Y., Di Renzo, M., ... & Cui, T. J. (2020). Wireless communications with reconfigurable intelligent surface: Path loss modeling and experimental measurement. *IEEE Transactions on Wireless Communications*.
19. Liu, Y., Ketterl, T. P., Arrobo, G. E., & Gitlin, R. D. (2014, December). Modeling the wireless in vivo path loss. In *2014 IEEE MTT-S International Microwave Workshop Series on RF and Wireless Technologies for Biomedical and Healthcare Applications (IMWS-Bio2014)* (pp. 1-3). IEEE.
20. Bok, J., & Ryu, H. G. (2014, February). Path loss model considering Doppler shift for high speed railroad communication. In *16th International Conference on Advanced Communication Technology* (pp. 1-4). IEEE.
21. Choudhary, S., & Dhaka, D. K. (2015). Path loss prediction models for wireless communication channels and its comparative analysis. *Int. J. Eng. Management & Sciences*, *2*(3), 38-43.
22. MacCartney, G. R., Samimi, M. K., & Rappaport, T. S. (2014, September). Omnidirectional path loss models in New York City at 28 GHz and 73 GHz. In *2014 IEEE 25th Annual International Symposium on Personal, Indoor, and Mobile Radio Communication (PIMRC)* (pp. 227-231). IEEE.
23. Sulyman, A. I., Alwarafy, A., MacCartney, G. R., Rappaport, T. S., & Alsanie, A. (2016). Directional radio propagation path loss models for millimeter-wave wireless networks in the 28-, 60-, and 73-GHz bands. *IEEE Transactions on Wireless Communications*, *15*(10), 6939-6947.
24. Haider, M. K., & Knightly, E. W. (2016, July). Mobility resilience and overhead constrained adaptation in directional 60 GHz WLANs: protocol design and system implementation. In *Proceedings of the 17th ACM International*

Symposium on Mobile Ad Hoc Networking and Computing (pp. 61-70).

25. Akdeniz, M. R., Liu, Y., Samimi, M. K., Sun, S., Rangan, S., Rappaport, T. S., & Erkip, E. (2014). Millimeter wave channel modeling and cellular capacity evaluation. *IEEE journal on selected areas in communications*, *32*(6), 1164-1179.
26. Fickenscher, T., & Raza, M. B. (2014, March). Diffraction loss and phase modulation of terrestrial radio-link by wind turbine. In *2014 International Workshop on Antenna Technology: Small Antennas, Novel EM Structures and Materials, and Applications (iWAT)* (pp. 382-384). IEEE.
27. Robaei, M., & Akl, R. (2021, May). Millimeter-wave blockage modeling and mitigation. In *2021 IEEE International Workshop Technical Committee on Communications Quality and Reliability (CQR 2021)* (pp. 1-6). IEEE.
28. Jude, O. O., Jimoh, A. J., & Eunice, A. B. (2016). Software for Fresnel-Kirchoff single knife-edge diffraction loss model. *Mathematical and Software Engineering*, *2*(2), 76-84.
29. Abdulrasool, A. S., Aziz, J. S., & Abou-Loukh, S. J. (2017). Calculation algorithm for diffraction losses of multiple obstacles based on Epstein–Peterson approach. *International Journal of Antennas and Propagation*, *2017*.
30. Nwokonko, S. C., Onwuzuruike, V. K., & Nkwocha, C. P. (2017). Remodelling of Lee's Knife Diffraction Loss Model as a Function of Line of Site Percentage Clearance. *International Journal of Theoretical and Applied Mathematics*, *3*(4), 138.
31. Nnadi, N. C., Nnadi, C. C., & Nnadi, I. C. (2017). Computation of diffraction parameter as a function of line of site percentage clearance. *Mathematical and Software Engineering*, *3*(1), 149-155.